Volume 11
Number 25
7 July 2020
Pages 6341–6592

Chemical Science

10TH ANNIVERSARY

rsc.li/chemical-science

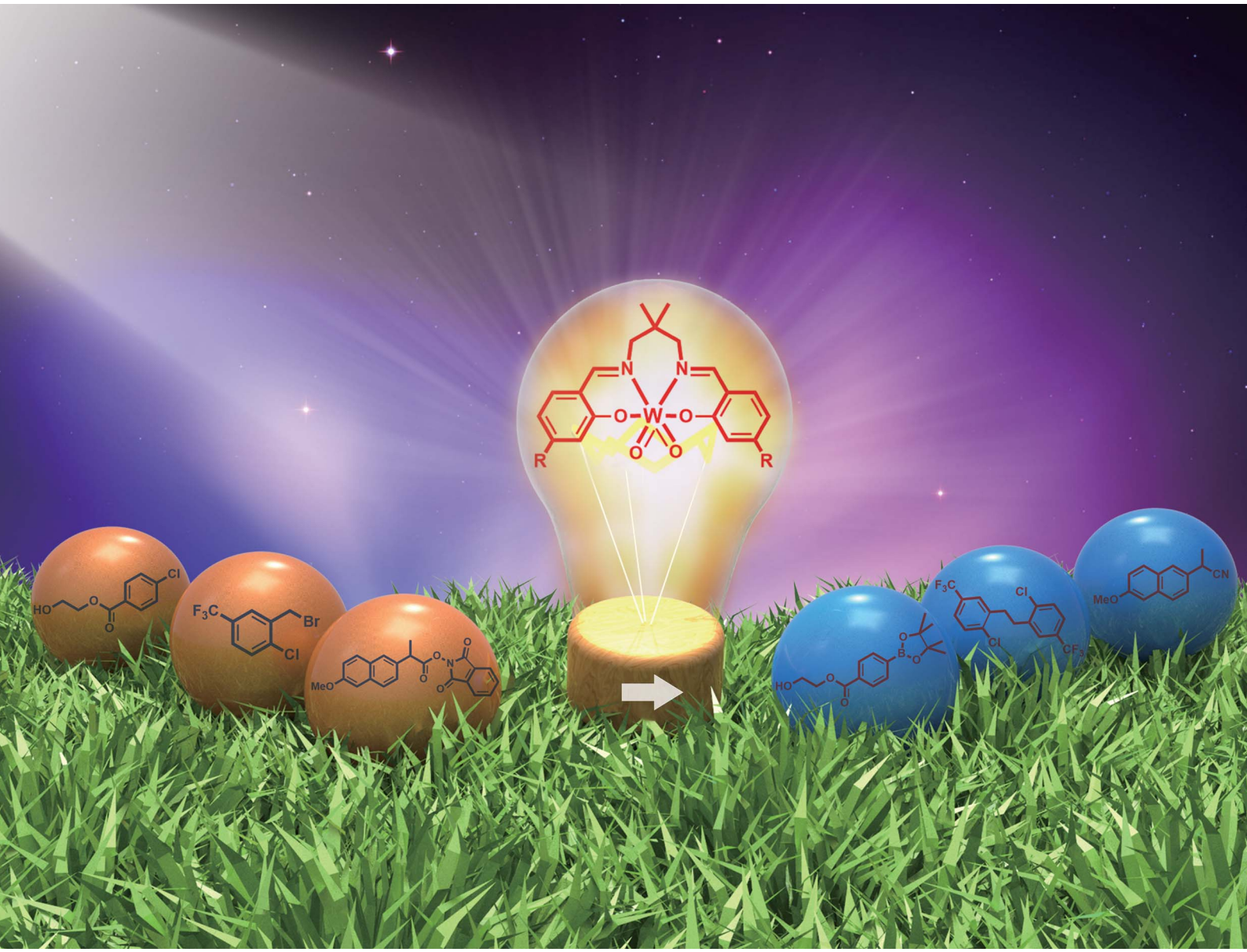

ISSN 2041-6539

ROYAL SOCIETY OF CHEMISTRY

EDGE ARTICLE
Chi-Ming Che *et al.*
Luminescent tungsten(VI) complexes as photocatalysts for light-driven C–C and C–B bond formation reactions

Chemical Science

ROYAL SOCIETY OF CHEMISTRY

EDGE ARTICLE

View Article Online
View Journal | View Issue

Cite this: *Chem. Sci.*, 2020, **11**, 6370

All publication charges for this article have been paid for by the Royal Society of Chemistry

Received 5th March 2020
Accepted 23rd May 2020

DOI: 10.1039/d0sc01340d

rsc.li/chemical-science

Luminescent tungsten(VI) complexes as photocatalysts for light-driven C–C and C–B bond formation reactions†

Daohong Yu,[ab] Wai-Pong To,[b] Glenna So Ming Tong,[b] Liang-Liang Wu,[b] Kaai-Tung Chan,[b] Lili Du,[b] David Lee Phillips,[b] Yungen Liu[a] and Chi-Ming Che*[abc]

The realization of photocatalysis for practical synthetic application hinges on the development of inexpensive photocatalysts which can be prepared on a large scale. Herein an air-stable, visible-light-absorbing photoluminescent tungsten(VI) complex which can be conveniently prepared at the gram-scale is described. This complex could catalyse photochemical organic transformation reactions including borylation of aryl halides, such as aryl chloride, reductive coupling of benzyl bromides for C–C bond formation, reductive coupling of phenacyl bromides, and decarboxylative coupling of redox-active esters of alkyl carboxylic acid with high product yields and broad functional group tolerance.

Introduction

Transition metal photocatalysis has become an intensively investigated area and has developed rapidly as a useful strategy for a broad range of organic transformations under mild conditions.[1] Most of the photocatalysts employed in these studies are usually based on platinum group metals such as Ru^{II} and Ir^{III} due to the efficient light-absorption properties of their complexes in the visible spectral region and accessibility to attain triplet excited states with a sufficient lifetime for bimolecular energy transfer and electron transfer reactions upon photo-excitation. Non-precious metal complexes such as those of Cu,[2] Ni,[3] Zr,[4] Mo,[5] Cr,[6] Fe,[7] and Ce[8] have also been studied and applied in light-driven organic transformation reactions. Meanwhile, earth-abundant tungsten(VI) oxides such as WO_3 and polyoxotungstate[9] display rich photoluminescence, an example of which is $(n\text{-}Bu_4N)_4[W_{10}O_{32}]$ photocatalysed C–H bond functionalization.[10] Nonetheless, tungsten oxide has low solubility in common organic solvents and the decatungstate anion only absorbs in the UV spectral region up to 400 nm.[11] In this regard, the design and modification of tungsten oxide coordinated with ligands are appealing. Tungsten, though having a large spin–orbit coupling constant ($\zeta = 2433\ cm^{-1}$) for efficient intersystem crossing from the singlet to the triplet excited state, has rarely been explored in the design of photofunctional molecular materials. In the literature, several luminescent W^0 isocyanides[12] have been found as "proof-of-concept" strong photo-reductants.

Recently, we reported air-stable luminescent W(VI) complexes and described their applications in organic light-emitting diodes as well as photo-sensitization of singlet oxygen and reduced oxygen species ($O_2^{\bullet-}$).[13] Herein the broad applications of W(VI) oxo complexes in visible-light driven coupling reactions for C–C bond formation are described. Given the ease of preparation and facile tuning of the photophysical properties of the Schiff base ligand scaffold, we further modified the structure of luminescent W(VI) Schiff base complexes to increase their absorption in the visible spectral region and to modulate the excited state reduction potential by introducing an electron-donating group into the ligand.[14,15] These complexes (Fig. 1, **W1a–W1c**) display photoluminescence with quantum yields of up to 0.13 and lifetimes of up to 83.6 μs in dichloromethane solution at room temperature. With these complexes as the photocatalyst, reactions such as borylation of

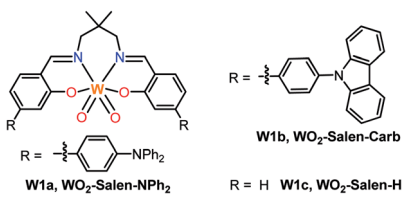

Fig. 1 Tungsten(VI) complexes **W1a–W1c** studied in this work.

[a]*Department of Chemistry, Southern University of Science and Technology, Shenzhen, Guangdong 518055, China. E-mail: cmche@hku.hk*

[b]*State Key Laboratory of Synthetic Chemistry, HKU-CAS Joint Laboratory on New Materials, Department of Chemistry, The University of Hong Kong, Pokfulam Road, Hong Kong, China*

[c]*HKU Shenzhen Institute of Research and Innovation Shenzhen, Guangdong 518055, China*

† Electronic supplementary information (ESI) available: Experimental details, photophysical data, DFT calculations and NMR spectral data. See DOI: 10.1039/d0sc01340d

aryl halides, including aryl chloride, and C–C reductive coupling of benzyl bromides were achieved in moderate to good product yields under blue LED light irradiation.

Results and discussion

Synthesis and characterization

Schiff base ligands were synthesized by condensation reaction of the respective salicylaldehyde with 2,2-dimethylpropane-1,3-diamine. Strongly electron-donating diphenylamine (–NPh_2) substituents are present on the phenoxide moiety of **W1a** so as to generate an intraligand charge transfer (ILCT) excited state with large molar absorptivity in the visible spectral region and with the photo-generated "hole" localized mainly on the –NPh_2 groups for improving the stability of the metal complex in the course of photocatalysis. The W(VI) complexes were synthesized by refluxing a mixture of the ligand and [W(eg)$_3$] (eg = 1,2-ethanediolato) in MeOH/$CHCl_3$ (v/v = 1 : 1) and obtained as a purified product in 68–90% yields. The synthesis of **W1a** could be scaled up to give 1 g of the target complex in a one-pot reaction. These complexes are air- and moisture-stable yellow solids. They exhibit good solubility in CH_2Cl_2, THF and DMF and excellent stability in these solvents in the absence of light. The photo-stability of these W(VI) complexes in DCM and DMF was examined. Light irradiation (450 nm LED) of **W1a** in [D_2]DCM or [D_7]DMF in the absence of oxygen for 48 hours led to a slight change in the ^{1}H NMR spectrum (Fig. S1†). However, **W1b** and **W1c** were found to decompose completely under the same conditions, suggesting that the presence of NPh_2 provides a higher photo-stability to **W1a**.

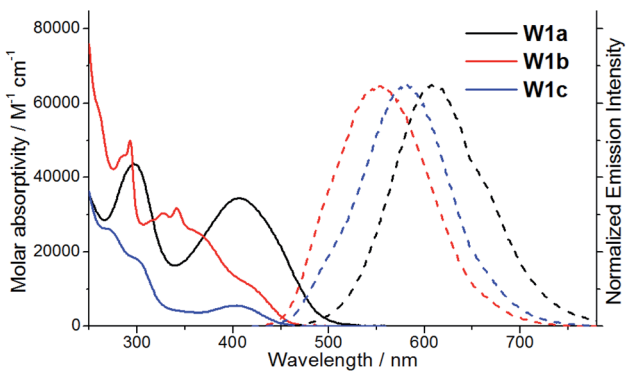

Fig. 2 UV-vis absorption (solid line) and emission (dashed line) spectra of **W1a–W1c** in degassed dichloromethane solutions at room temperature.

Spectroscopic and photophysical properties

The spectroscopic and excited state properties of these W(VI) complexes have been examined (Table 1 and S1†). In CH_2Cl_2, complex **W1a** shows two intense (3.84–4.98 × 10^4 M^{-1} cm^{-1}), broad absorption bands with maxima at 297 and 407 nm, the latter of which ends at ~510 nm, while **W1b** and **W1c** exhibit intense (1.82–5.71 × 10^4 M^{-1} cm^{-1}) absorption bands at 250–320 nm and a relatively weak band (5.5–11.4 × 10^3 M^{-1} cm^{-1}; shoulder for **W1b**) at 402–420 nm (Fig. 2). Complex **W1b** exhibits additional vibronic-structured absorption at ~290 and 340 nm, ascribable to the absorption of the carbazole unit on the ligand. These absorption bands are assigned to the ^{1}IL (singlet intraligand) transitions of the ligands, whereas the intense absorption band of **W1a** at 407 nm is proposed to have significant ILCT characteristics due to the electron-rich diphenylamine unit on the ligand. The strong absorptivity of **W1a** at a wavelength >400 nm is advantageous for this complex to catalyse visible light driven reactions when compared to **W1b** and **W1c**. Upon light excitation, **W1a** exhibits a broad, structureless emission with a peak maximum at 608 nm and with an emission quantum yield of 0.11 and lifetime of 4.6 μs. **W1b** and **W1c** exhibit photoluminescence with quantum yields of 0.13 and 0.03, respectively, and much longer emission lifetimes of 74.9 and 83.8 μs, respectively. The much higher emission quantum yields of **W1a** and **W1b** compared to **W1c** indicate that installing an amino substituent at the 4-position of the phenolate moiety can enhance the photoluminescence quantum yield of this class of complexes. While their emission profiles appear broad and structureless, a shoulder can be observed at ~500 nm. By examining their emission in aerated solutions (Fig. 3), it was found that these complexes exhibit prompt fluorescence which appears as a broad band with peak maxima at 509 and 513 nm, respectively. Their fluorescence emission quantum yields are estimated to be 0.006 and 0.001, respectively. The excitation spectra obtained at these emission wavelengths are highly similar to the absorption spectra of the respective complexes, confirming that this fluorescence originates from the W(VI) complexes (Fig. S3†). The long emission lifetimes of **W1b** and **W1c** also render their phosphorescence completely quenched under aerated conditions. Together with the minor solvent effect (<7 nm) on the emission for **W1b** and

Table 1 Photophysical data of complexes **W1a–W1c** in CH_2Cl_2[a]

	Absorption	Emission
	λ_{abs} [nm] (ε [×10^3 mol^{-1} dm^3 cm^{-1}])[a]	λ_{em} [nm] (Φ; τ [μs]; k_r [10^3 s^{-1}])
W1a[b]	297 (43.7), 407 (34.6)	608 (0.11; 4.6; 23.9)[b]
W1b	261 (57.1), 285 (45.9), 292 (49.8), 327 (30.4), 341 (31.9), 365 (sh, 25.0), 420 (sh, 10.6)	553 (0.13; 74.9; 1.7)
W1c[b]	270 (26.2), 299 (18.2), 402 (5.5)	582 (0.03; 83.6; 0.4)[b]

[a] Data were measured in degassed CH_2Cl_2 at 298 K. Emission quantum yields (Φ) were estimated with [Ru(2,2′-bipyridine)$_3$](PF$_6$)$_2$ in degassed CH_3CN as the standard (Φ = 0.062). The radiative decay rate constant is estimated using $k_r = \Phi/\tau$. [b] Values taken from ref. 15.

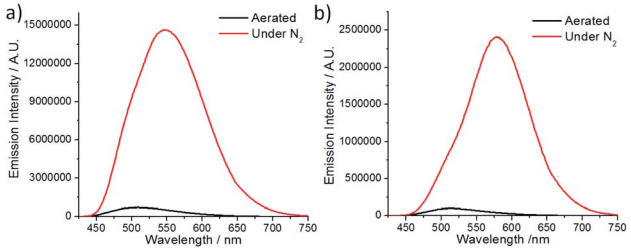

Fig. 3 Emission spectra of (a) **W1b** and (b) **W1c** in CH_2Cl_2 under aerated conditions and under N_2.

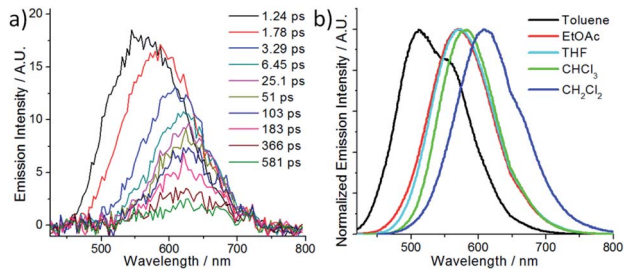

Fig. 4 (a) Femtosecond time-resolved emission spectra of **W1a** in CH_2Cl_2 and (b) emission of **W1a** in different solvents (adapted with permission from ref. 15. Copyright 2019, Wiley-VCH Verlag GmbH & Co. KGaA).

W1c (Table S1†), the emissions of **W1b** and **W1c** originate from ^{3}IL excited states. For **W1a**, a broad emission band with a peak maximum at 605 nm and an emission lifetime of 0.54 μs was observed under aerated conditions, implying that its emission was not completely quenched in the presence of dissolved oxygen (Fig. S4†). Femtosecond time-resolved emission (fs-tre) measurements (Fig. 4a) revealed that **W1a** shows a broad, structureless fluorescence peak with the peak maximum at ~560 nm at the early stage (within 1 ps); this fluorescence then showed a dynamic Stokes shift to ~620 nm in about 3 ps and decayed with a time constant of 324 ps. The steady state emission of **W1a** exhibits significant positive solvatochromism (λ_{max} = 510 nm in toluene, 572 nm in THF, and 608 nm in CH_2Cl_2; Fig. 4b and Table S1†), and the emission quantum yield and lifetime of **W1a** even reach 0.28 and 22.1 μs in degassed $CHCl_3$. The positive solvatochromism is suggestive of substantial charge-transfer characteristics in its emissive excited state and its emission in toluene originates predominantly from the ^{3}ILCT excited state according to the DFT calculation in our previous work.[15] In toluene, **W1a** shows a structured emission with the peak maximum at 510 nm and a shoulder at 552 nm with a quantum yield and lifetime of 0.04 and 67.6 μs, respectively, which corresponds to a radiative decay rate constant (k_r) of 600 s^{-1}. But upon changing the solvent to $CHCl_3$ and CH_2Cl_2, its emission maximum red-shifts to 583 and 608 nm, and k_r increases to 1.27×10^4 and 2.39×10^4 s^{-1}, which are, respectively, 21 and 40 times larger than those in toluene (Table S1†). Such an increase in k_r implies a change in the emission origin to a faster radiative decay mechanism, possibly with the involvement of TADF.[15] A similar emission peak maximum observed

Table 2 Electrochemical properties and excited state potentials of W1a–W1c[a]

Complex	E_{pc}/V	E_{pa}/V	E_{0-0}/eV	$E(W^*/W^-)$	$E(W^+/W^*)$
W1a	−1.29[b]	+1.10[b]	2.39	+1.10	−1.29
W1b	−1.24	+1.41	2.70	+1.46	−1.29
W1c	−1.34[b]	+1.64[b]	2.59	+1.25	−0.95

[a] Values *vs.* SCE. [b] Values taken from ref. 15.

with fs-tre (~620 nm), which represents the $S_1 \rightarrow S_0$ prompt fluorescence, and steady state emission measurement (608 nm) also support such a possibility. It is noted that although both **W1a** and **W1b** are appended with amino-substituents, **W1a** exhibits an emission with a larger k_r of 2.39×10^4 s^{-1} and with the involvement of TADF while **W1b** displays long-lived ^{3}IL emission. One possible reason accounting for this difference is the much higher-lying HOMO of **W1a** (0.31 V higher than that of **W1b**; Table 2) resulting in the $^{1/3}$ILCT excited states being lower-lying than the ^{3}IL excited state. A similar finding for the difference in the luminescence properties between complexes having carbazole and diphenylamine, respectively, was observed in pincer Au(III) aryl complexes as well.[16]

DFT/TDDFT calculations

In most cases, the charge transfer absorption band is usually weak due to spatial separation of the donor and acceptor orbitals which minimizes the overlap between the two wavefunctions, and hence the transition dipole moment.[15] However, it is observed herein that the first absorption peak of **W1a**, which has been assigned as derived from the $S_0 \rightarrow {}^1$ILCT transition, is rather intense (ε in the order of 10^4 M^{-1} cm^{-1}). This seems quite unusual, especially when compared with the first absorption peak of **W1c**, which has been assigned to the $S_0 \rightarrow {}^1$IL transition with ε in the order of 10^3 M^{-1} cm^{-1}. Time-dependent density functional theory (TDDFT) calculations at their respective optimized S_0 geometries have been performed to understand this phenomenon. The computed first absorption band is at 370 and 390–443 nm in toluene for complexes **W1c** and **W1a**, respectively, which is in reasonable agreement with the experimentally observed absorption band (Fig. S15† displays the simulated absorption spectra of **W1a** and **W1c**). In particular, the computed first absorption band of **W1a** is more intense than that of **W1c**, as reflected by the absorption band oscillator strengths (f = 0.078 and 0.31–0.49 for **W1c** and **W1a**, respectively), which is also in line with experimental observations. These lend support to the reliability of the computational results for rationalization of the experimental data. The energy of the oxide(O^{2-})-to-tungsten charge transfer (LMCT) transition of **W1c** and **W1a** was estimated using TDDFT calculations at their respective optimized ground state geometry. It was found that the $S_0 \rightarrow {}^1$LMCT excitation is at 283 nm in toluene for both complexes, which is in agreement with the excitation λ_{max} of $[WO_2X_4]^{2-}$ at ~250–320 nm (X = Cl and F).[17]

The intensity of an absorption band intimately depends on the transition dipole moment (M) between the ground state and the excited state (say, S_n),

$$M(S_0 \rightarrow S_n) = \int T(r)(-er)\mathrm{d}r$$

$T(r)$ is the transition density of the $S_0 \rightarrow S_n$ transition, r is a point in three-dimensional space, and e is the electronic charge. The transition density $T(r)$ is related to the overlap density between the two MOs (φ_i and φ_a) involved in an excitation:

$$T(r) = \sum_i \sum_a w_i^a \varphi_i(r)\varphi_a(r)$$

w_i^a is the contribution of the $\varphi_i \rightarrow \varphi_a$ excitation, and the summation is run over all the (i,a) MO pairs of excitation in an electronic transition (i is the index for occupied MOs and a is the index for unoccupied MOs). Thus, there are two parameters that control the magnitude of M, the distance r and the orbital overlap. For **W1c**, the lowest energy absorption band is predominantly derived from the $S_0 \rightarrow S_1$ excitation and is composed mainly of the HOMO → LUMO transition where both the HOMO and LUMO have substantial contributions from the Schiff base ligands (91% and 70% for the HOMO and LUMO, respectively; see Fig. S18†). Thus, the HOMO–LUMO overlap is large (0.623), as expected for IL transition. On the other hand, for **W1a**, the first absorption band is composed of excitations from the ground state to the S_1, S_2, and S_3 excited states (Fig. S15†). These excitations are mainly derived from H−1 → LUMO (86%, S_1), HOMO → LUMO (86%, S_2), and HOMO → L+1 (92%, S_3) transitions; HOMO and H−1 are mainly localized on the triphenylamine (TPA) moieties (93–95%) while LUMO and L+1 are dominantly localized on the Schiff base ligands (77–79%; Fig. S17†). These transitions are thus termed ILCT and the orbital overlap is expectedly smaller (0.149–0.352).

Since the transition dipole moment also depends on r, it may be more intuitive to compare the transition dipole moment density (TDMD), $T(r)$ r and the fragment transition dipole moment (TDM) which is the spatial integrals of the TDMD of the fragment. Fig. 5 depicts the TDMD and fragment TDM along the z-direction of the $S_0 \rightarrow S_1$ excitation. Attaching TPA to the Schiff base ligands extends the transition density distribution onto the TPA ligand, leading to an increase in the TDMD and a substantial fragment TDM at the TPA moieties (−0.086 and 0.916 a.u. for **W1c** at the Schiff base ligand and 0.516 and −3.23 a.u. at the TPA moieties for **W1a**). Similarly, the TDMD and the fragment TDM of the $S_0 \rightarrow S_2$ and $S_0 \rightarrow S_3$ excitations have substantial contributions at the TPA moieties of **W1a**. (Fig. S19 and S20†) Thus, increasing the donor–acceptor distance while maintaining significant transition density could lead to substantial enhancements of the $S_0 \rightarrow S_n$ intensities, which accounts for the intense absorption of **W1a**.

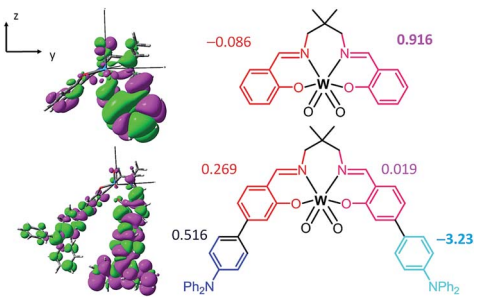

Fig. 5 Transition dipole moment density (left) and the fragment transition dipole moment (right) along the z-direction of the $S_0 \rightarrow S_1$ excitation in toluene solution at the respective optimized S_0 geometries of **W1c** (top) and **W1a** (bottom). Colour code: magenta, negative; green, positive; isovalue = 0.001 a.u.

Excited state dynamics

The early events of excited state dynamics have been probed by femtosecond time-resolved absorption (fs-ta) spectroscopy. As portrayed in Fig. 6a, the fs-ta spectrum obtained for **W1a** in CH_2Cl_2 at various time intervals after laser excitation (400 nm) evolved from having an absorption difference peak maximum at ~480 nm and shoulder at 570 nm to a broad absorption profile spanning from 500 to 750 nm with a time constant of 370 ps, the latter of which is close to the fs-tre decay time constant (τ_{620nm} = 324 ps). Excitation at 266 nm gave similar spectral evolution (Fig. S7†). For **W1b**, the fs-ta spectra recorded within 10 ps show a peak maximum at ~470 nm and a broader absorption band covering 550–700 nm (Fig. 6b). Then, the absorption difference at ~470 nm decreases while that at 500–700 nm grows with a time constant of 83 ps. For **W1c**, at 1.9 ps after laser excitation, the fs-ta spectrum shows a peak maximum at ~480 nm and a broad, less intense absorption band beyond 650 nm (Fig. S8†). The spectrum then evolves with a time constant of 42 ps to generate a new profile with a broader absorption band with the peak maximum at ~490 nm and a weaker, broad absorption band beginning at ~570 nm. Since the final spectral profiles observed in these fs-ta spectra highly resemble those obtained in ns-ta spectra (Fig. S6†), these spectral transformations are ascribed to intersystem crossing (ISC) from S_1 to the triplet manifold. The ISC time constants of 10^1–10^2 ps observed for these complexes are of the same order of magnitude as reported for the W(VI) Schiff base dioxo complexes.[13,15] However, these ISC time constants are quite large when compared to those of Pt(II) and Au(III) complexes which usually lie in the range of 0.1 to a few ps.[18] These slow ISC time constants also account for the observation of fluorescence bands of **W1b** and **W1c** in steady state emission measurements. For **W1a**, since the ILCT excited state would lead to a small energy difference between the S_1 and

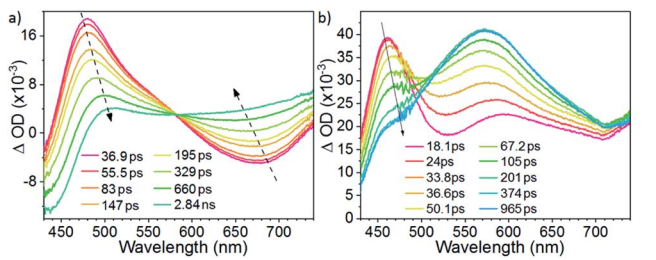

Fig. 6 fs-TA spectra of (a) **W1a** and (b) **W1b** in CH_2Cl_2 at room temperature.

T_1 excited states, the emission originating from these two states have significant spectral overlap and the prompt fluorescence band (~560–620 nm) could only be observed with femtosecond time-resolved emission spectroscopy (Fig. 4a).

Electrochemistry and excited state redox potentials

The electrochemical properties of these complexes have been examined by cyclic voltammetry in DMF containing 0.1 M nBu$_4$NPF$_6$ as the electrolyte. These complexes exhibit an irreversible ligand-centred reduction wave at −1.24 to −1.34 V *vs.* SCE and an irreversible ligand-centred oxidation wave at +1.10, +1.41 and +1.64 V *vs.* SCE for **W1a**, **W1b** and **W1c**, respectively. The reduction wave of **W1a** remains irreversible even at a scan speed of 1 V s^{-1}, suggesting that the reduced form of **W1a** has limited stability under electrochemical conditions (Fig. S13†). The increasing ease of oxidation on moving from **W1c** to **W1a** is ascribed to the presence of electron-donating carbazole and diphenylamine groups on their respective phenoxide moieties. The E_{0-0} values of **W1a**, **W1b** and **W1c** are estimated to be 2.39, 2.70 and 2.59 eV, respectively, accordingly to the onset of their triplet emission in MeCN. By combining their spectroscopic and electrochemical data, the excited state reduction potentials [E(W*/W$^-$)] of **W1a**, **W1b** and **W1c** were estimated to be +1.10, +1.46 and +1.25 V *vs.* SCE, respectively (Table 2), indicating that these tungsten complexes are good photo-oxidants. The redox potentials [E(W$^+$/W*)] are estimated to be −1.29, −1.29 and −0.95 V *vs.* SCE, respectively, which denotes the reducing nature of their excited states.

Photocatalysis

We first examined the feasibility of the W^{VI}-oxo complex to perform photochemical dehydrogenation of alcohols by photolysis of **W1a** in the presence of secondary alcohol substrates. It was found that 1-indanol and 1-phenylethanol could be oxidized to the corresponding ketones in 52% and 16% yields, respectively, after 12 hours of light irradiation with LEDs (365 nm) (Scheme 1; Table S3†). No reaction was observed in the absence of oxygen. Changing the light source to 450 nm LEDs resulted in only 15% and 9% conversion of these alcohols to ketones, suggestive of the need for high-energy excitation for efficient dehydrogenation of benzyl alcohols. Cyclohexa-1,4-diene and Hantzsch ester, which have much weaker C–H bonds, were readily converted to benzene and the corresponding pyridine in almost quantitative yields (Scheme 1).

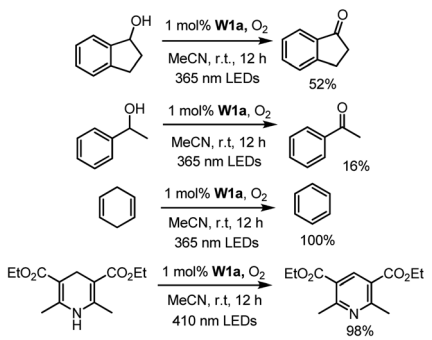

Scheme 1 Photo-induced dehydrogenation reactions catalysed by W1a.

Next, we examined the catalytic activity of these complexes in photo-redox reactions. Aryl boronic acid and esters are important building blocks for the formation of aryl carbon–carbon or carbon-heteroatom bonds.[19] Recently, a number of strategies for photo-induced borylation of aryl halides *via* direct ultraviolet light irradiation,[20] in the presence of a metal-based photocatalyst[8i,21] or *in situ* generated electron donor[21] have been developed. At the outset, visible-light-induced borylation of 1-iodo-3,5-dimethylbenzene with bis(pinacolato)-diboron (B_2Pin_2) was chosen as a model reaction with the most commonly used Hunig base (DIPEA) as a reductive quencher. To our delight, the borylation of aryl iodide proceeded smoothly and gave the desired product in 52% yield together with *m*-xylene derived from the hydrodehalogenation of aryl halide as the major by-product. Other reaction parameters such as the base, additive, and solvent were further optimized (see Table S4† for details). Meanwhile, we discovered that the reaction protocol was also applicable to aryl bromide and aryl chloride, the latter of which was recently reported to be an effective substrate in photo-redox reactions.[8i,22] The reaction of ethyl 4-chlorobenzoate (**1b**) and B_2Pin_2 under the same conditions afforded the desired product **2b** in 53% yield and the by-product ethyl benzoate in 41% yield (Table S5,† entry 1). Further screening of reaction conditions revealed that when tetrabutylammonium bromide (TBAB) or TBAB/KI was used, the formation of the dehalogenated by-product was suppressed efficiently (Table S5,† entry 15, 16) to ≤9%. In the absence of a photosensitizer, the product yield was greatly reduced to 20%, indicative of the role of **W1a** in increasing the efficiency of the reaction (Table S5,† entry 17). The reaction conducted in the absence of light did not show conversion of the substrate, confirming that visible light is critical to the reaction (Table S5,† entry 18). Under the same conditions, low product yields of 14–30% were obtained when using **W1b** and **W1c** as the catalyst.

With the optimal conditions, we explored the substrate scope of the borylation reaction with aryl halides (Table 3). Reactions of aryl chlorides with an electron-withdrawing group such as ester, amide, ketone and nitrile proceeded smoothly to give the corresponding products in good to excellent yields (Table 3, **2b–c**, **2f–h**). This borylation reaction showed good tolerance to various functional groups such as free alcohol and alkyl bromide (Table 3, **2i**, **2l**). Sterically hindered aryl chloride could also give the corresponding product in 81% yield (Table 3, **2j**). However, substrates with methyl substituent(s) generally gave a moderate yield (50–66%) of products (Table 3, **2a**, **2m–o**). The reaction of alkyl halides under the same reaction conditions has also been examined. When 2-(bromomethyl)-1-chloro-4-(trifluoromethyl)benzene (**3i**) was subjected to the borylation reaction, the borylated product was not detected. Instead the 1,2-diphenylethane product was isolated in high yield (Table 4, **4i**). The reductive homocoupling reaction of benzyl halides has been reported.[2b,c,8a,23,24] In this work, reductive coupling of benzyl bromide occurred smoothly to give the dimerization product, 1,2-diphenylethane, under similar reaction conditions

Table 3 Photo-induced borylation of aryl halides catalysed by **W1a**[a]

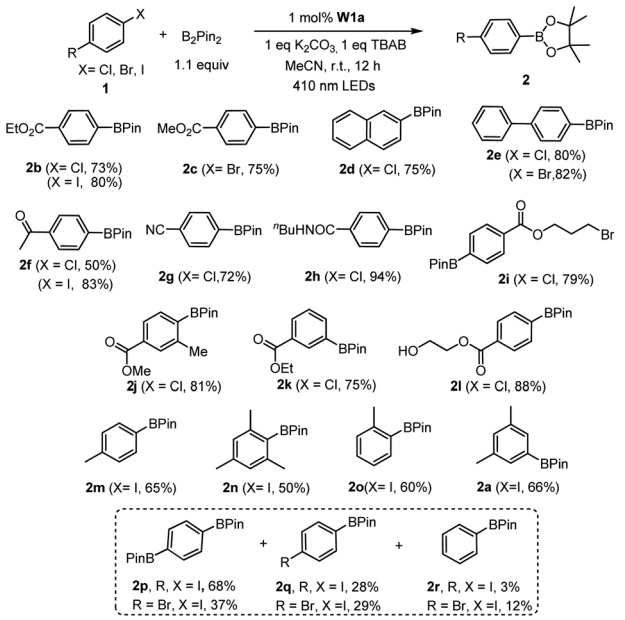

[a] Reaction conditions: **1** (0.5 mmol), B_2Pin_2 (0.55 mmol), **W1a** (1 mol%), K_2CO_3 (0.5 mmol), TBAB (0.5 mmol) in MeCN and irradiated using 410 nm LEDs at room temperature for 12 h. Isolated yields.

Table 4 Photo-induced C–C bond coupling reaction of benzylic halides catalysed by **W1a**[a]

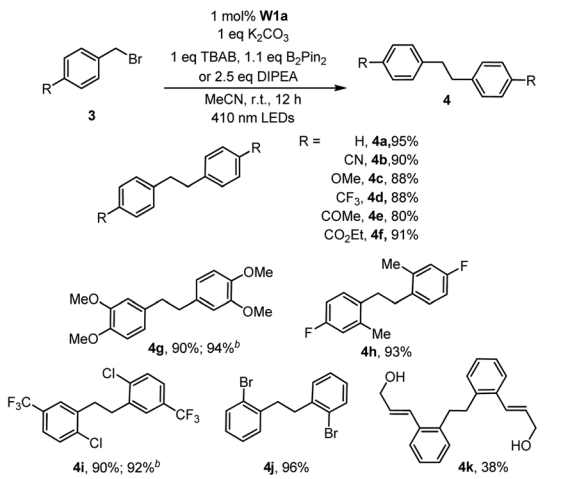

[a] Reaction conditions: **3** (0.5 mmol), B_2Pin_2 (0.55 mmol), **W1a** (1 mol%), K_2CO_3 (0.5 mmol), TBAB (0.5 mmol) in MeCN and irradiated using 410 nm LEDs at room temperature for 12 h. Isolated yields. [b] TBAB and B_2Pin_2 replaced with DIPEA.

(Table 4). Interestingly, although no borylation product was found in the reaction mixture, the presence of B_2Pin_2 is critical for the photo-redox reaction, without which the yield of the desired coupling product decreased dramatically to 30%. After further screening, we discovered that the use of DIPEA instead of the combination of TBAB and B_2Pin_2 gave slightly higher product yields of **4g** and **4i**. Both methods are effective for the reductive coupling reaction of benzyl bromide. A variety of benzyl bromides with electron-withdrawing groups or electron-donating groups delivered the products in 80–95% yields (Table 4, **4a–g**). As for the substrate having both benzylic and arylic bromide groups, benzylic bromide showed its priority in the reaction (Table 4, **4j**).

The capacity of **W1a** in catalysing the reductive dehalogenation of arylacyl bromide which has been reported by other groups[25] was also examined (Table 5). 1,4-Dicarbonyl compounds were obtained in 74–94% yields, presumably due to the absence of a proton source in the reaction. When cinnamyl bromide was used, the dimerized product was obtained in 73% yield, with the ratio of isomer products being about 1 : 0.6 : 0.1.

Redox-active esters[26] (RAEs; *e.g.* *N*-hydroxyphthalimide ester **5**) derived from alkyl carboxylic acid as convenient surrogates for alkyl halides were examined for the generation of alkyl radicals which could be trapped with various reagents (*e.g.* diselenide,[27] Michael acceptors,[26e,28] CCl_4,[29] 1-bromocarbagermatranes[30] and benzophenone imine[31]). In this work, the light-induced decarboxylative radical addition reaction of redox-active esters in the presence of styrene or acrylate ester was examined. No radical addition product was detected in the presence of **W1a** and DIPEA. Different from most related literature reports, we found that the light-induced decarboxylative coupling reaction occurred to give sterically hindered 1,2-diphenylethanes (Table 6).[32] Decarboxylative coupling products, including those having Cl and F substituents, could be obtained in 50–95% yields. Alkene groups were tolerated albeit at low yield (41%) due to the formation of the decarboxylative hydrogenation product.

Recently, Liu group reported that benzyl radicals generated from *N*-hydroxylphthalimide ester can be trapped by a reactive copper(II) cyanide to deliver benzyl nitriles.[33] Since our tungsten system could provide benzyl radicals *via* light irradiation, the decarboxylative cyanation of redox-active esters employing cooperative tungsten photocatalysis and copper catalysis was

Table 5 Photo-induced C–C bond coupling reaction of arylacyl bromides catalysed by **W1a**[a]

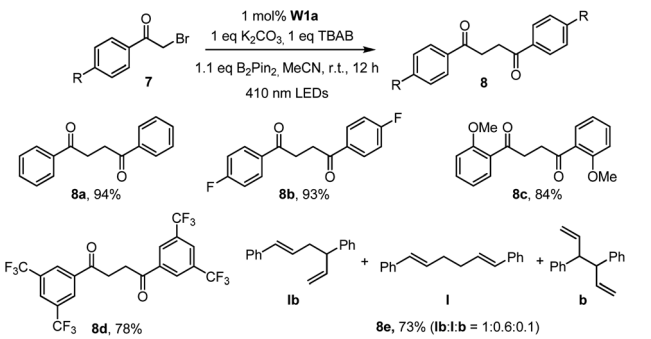

[a] Reaction conditions: **7** (0.5 mmol), B_2Pin_2(0.55 mmol), **W1a** (1 mol%), K_2CO_3 (0.5 mmol), TBAB (0.5 mmol) in MeCN and irradiated using 410 nm LEDs at room temperature for 12 h. Isolated yields.

Table 6 Photo-induced decarboxylative coupling reaction of redox-active esters catalysed by **W1a**[a]

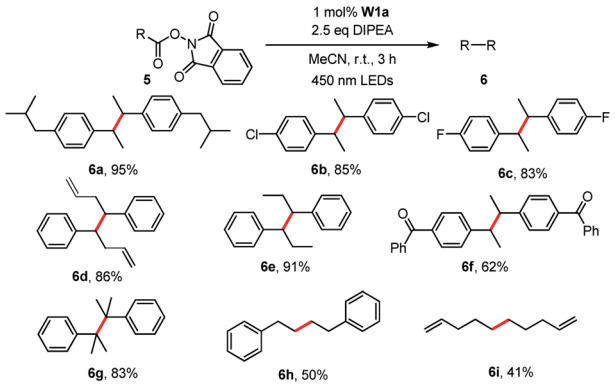

[a] Reaction conditions: **5** (0.5 mmol), **W1a** (1 mol%), DIPEA (1.25 mmol) in MeCN and irradiated using 450 nm LEDs at room temperature for 3 h. Isolated yields.

Table 7 Photo-induced decarboxylative cyanation reaction of redox-active esters catalysed by **W1a**[a]

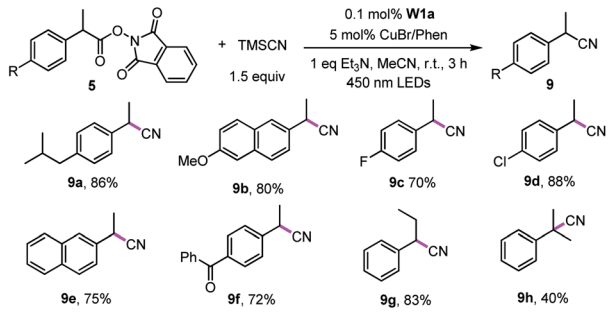

[a] Reaction conditions: **5** (0.5 mmol) **W1a** (0.1 mol%), TMSCN (0.75 mmol), CuBr (5 mol%), Phen (5 mol%), Et_3N (0.5 mmol) in MeCN and irradiated using 450 nm LEDs at room temperature for 3 h. Isolated yields.

examined (Table 7). Thus, various redox-active-esters derived from simple carboxylic acids were found to provide the corresponding nitrile products in good yields (72–88%) in the presence of only 0.1 mol% **W1a**. Quaternary benzyl nitrile, which could not be obtained in Liu's catalytic system, was furnished using our protocol in 40% yields.

During the study on the C–B bond formation reaction (Table 3), we observed the formation of dehalogenated by-products. In the literature, there are a number of examples on light-induced hydrodehalogenation of aryl halides.[14,34] Here, by simply removing B_2Pin_2 from the reaction conditions, the reductive dehalogenation of aryl halides occurred smoothly with good to excellent yields (Table 8). A panel of functional groups such as ester, ketone, cyano, amide and alcohol were tolerated. The reaction was not sensitive to steric hindrance. *Ortho* or *meta* substituted aryl chloride delivered the corresponding product in 80–85% yields. In the presence of aryl bromide and chloride, the aryl bromide was reduced preferentially with 85% yield

Table 8 Photo-induced dehalogenation of aryl halides catalysed by **W1a**[a]

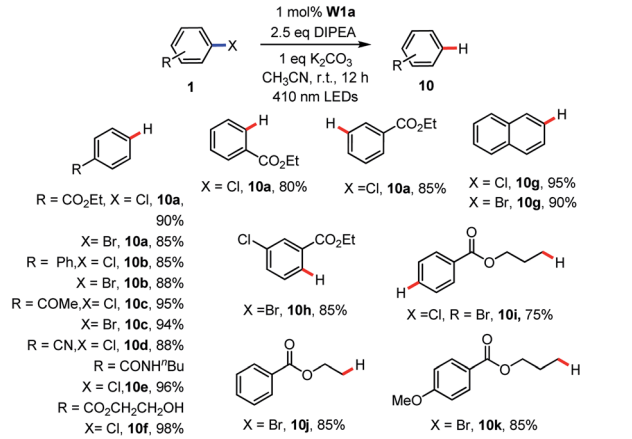

[a] Reaction conditions: **1** (0.5 mmol), **W1a** (1 mol%), DIPEA (1.25 mmol), K_2CO_3 (0.5 mmol) in MeCN at room temperature and irradiated using 410 nm LEDs for 3 h. Isolated yields.

while the chloride remained intact. In particular, alkyl bromides were reduced to afford the hydrodehalogenated product in 75–85% yields (**10i–10k**). When the substrate 3-bromopropyl 4-chlorobenzoate which contains aryl chloride and alkyl bromide in the same molecule was used, double reductive dehalogenation occurred to give propyl benzoate (**10i**) in 75% yield.

Photo-induced decarboxylative alkylation of silyl enol ether was reported to give aryl alkyl ketones with *N*-(acyloxy)phthalimide serving as the alkyl radical source.[35] Inspired by this work, we attempted tungsten catalysed alkylation of silyl enol ether with benzyl bromide. Instead of the expected product, bibenzyl and pinacol products (2,3-diphenylbutane-2,3-diol) were detected by GC-MS and ^{1}H NMR spectroscopy. Interestingly, in the absence of benzyl bromide, pinacol product **12a** was obtained in 94% yield (Table 9). Silyl enol ethers of acetophenone with methyl or trifluoromethyl groups afforded the corresponding products in 72% and 52% yields, respectively. While the mechanism of the homocoupling reaction of silyl enol ether to

Table 9 Photo-induced homocoupling reaction of silyl enol ethers catalysed by **W1a**[a]

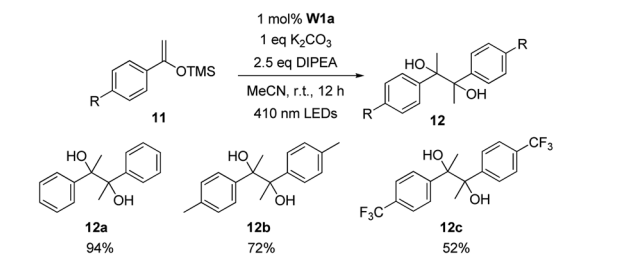

[a] Reaction conditions: **11** (0.5 mmol), **W1a** (1 mol%), DIPEA (1.25 mmol), K_2CO_3 (0.5 mmol) in MeCN at room temperature and irradiated using 410 nm LEDs for 12 h. Isolated yields.

give pinacol is not clear, the ketyl radical[36b–d] is speculated to be involved in the reaction. It is noted that the light-induced reductive homocoupling reaction of benzaldehyde or acetophenone to synthesize pinacol has been reported in recent years.[14,34i,36]

Mechanistic study

Several reactions shown in Fig. S10† were carried out to gain insights into the reaction mechanism. Firstly, when TEMPO (2,2,6,6-tetramethyl-1-piperidyloxy) as a radical scavenger was added to the reaction mixture for photo-induced homocoupling reaction of benzyl bromide (Table 4), the dimerization reaction was inhibited completely, and a new product, derived from trapping of the benzylic radical by TEMPO, was obtained in 73% yield (Fig. S10a†). Secondly, when the photo-induced homocoupling reaction of benzyl bromide was performed under an O_2 atmosphere, benzyl benzoate **6** and benzaldehyde were detected by GC-MS as the major product, the formation of which indicated the generation of benzyl radicals during the reaction (Fig. S10b†).[2b,37] Thirdly, a competitive reaction performed using an equivalent mixture of benzyl bromide with an electron-rich group (1-(bromomethyl)-4-methoxybenzene **3c**) and benzyl bromide with electron-withdrawing group (ethyl 4-(bromomethyl)benzoate **3e**) was found to give cross-over coupling product **4l** in 10% yield (Fig. S10c†). When a mixture of two benzyl bromides with electron-donating groups such as 1-(bromomethyl)-4-methoxybenzene **3c** and 4-(bromomethyl)-1,2-dimethoxybenzene **3g** was subjected to the reaction, the cross-over product **4m** was isolated in 40% yield (Fig. S10d†). The cross-over experiments indicated that the major product originated from a more stable radical intermediate. Fourthly, in the presence of styrene, the reductive coupling product **4f** (Table 4) was also obtained in 46% yield (Fig. S10e†). However, in contrast to the traditional photo-induced reaction in the presence of alkene or alkynes, the expected radical addition product[38] was not detected by GC-MS and ^{1}H NMR spectroscopy. DFT calculations revealed that the homocoupling reaction between two benzyl radicals is barrierless with a large driving force (ΔG) of −42.3 kcal mol^{-1}, whereas the radical addition to styrene is less prevalent with a barrier of 8.4 kcal mol^{-1} (Fig. S21†).

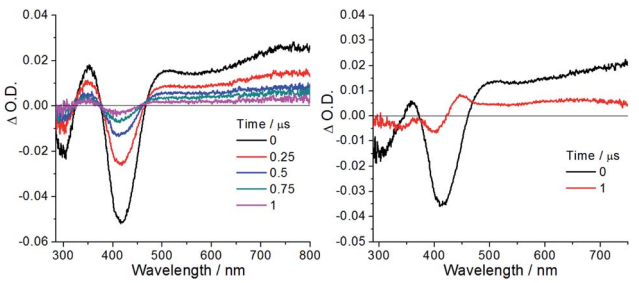

Fig. 7 Nanosecond time-resolved absorption difference spectra of (left) **W1a** only and (right) **W1a** in the presence of *N*,*N*-diisopropylethylamine (0.02 M) in degassed CH_3CN at room temperature.

For the role of the W(VI) complex in the catalysis, the Stern–Volmer emission quenching experiment demonstrated that the emission of **W1a** was quenched by DIPEA with a quenching rate constant (k_q) of 8.2 × 10^7 dm^3 mol^{-1} s^{-1}, together with the formation of a new absorption profile with a lifetime of 10.1 μs in ns-ta measurement (Fig. 7), while emission quenching was not observed with benzyl bromide. Since the oxidation of DIPEA by triplet excited **W1a** is thermodynamically favourable (E(**W1a***/**W1a**$^-$) = +1.10 V *vs.* SCE; E(DIPEA$^{+/0}$) = +0.81 V *vs.* SCE), the observed emission quenching is ascribed to the reductive quenching of **W1a** by DIPEA. With the addition of benzyl bromide, the new transient absorption profile was found to exhibit a faster decay lifetime of 5.1 μs (*vs.* 10.1 μs), suggesting that the proposed **W1a**$^{\bullet-}$ species generated *via* reductive quenching with DIPEA may react with benzyl bromide. Besides, electrochemical measurements revealed that an enhanced current was observed at the 1st reduction wave (E_{pc} = −1.29 V *vs.* SCE) of **W1a** upon addition of benzyl bromide, supporting that the one-electron reduced **W1a** could react with benzyl bromide (Fig. S9†).

Based on the aforementioned findings, a plausible mechanism was proposed. In the excited state, **W1a*** accepts an electron from an electron-donor (**D**) such as DIPEA to form a reduced species, **W1a**$^{\bullet-}$. Spin density calculations for **W1a**$^{\bullet-}$ reveal that the unpaired electron mainly resides on the imine ligand rather than the W=O moiety (Fig. S22†). The delocalized spin population also helps to hamper further interaction between **W1a**$^{\bullet-}$ and the benzyl radical to form the plausible tungsten-oxo adducts. Therefore, the one-electron reduced **W1a**$^{\bullet-}$ is proposed to serve as a reductant to react with substrates (benzyl halides) to generate the reactive radical and an anion (X^-) accompanied by the regeneration of **W1a**. The reactive radical species could be trapped by terminal reagents to yield the coupling products.

To gain insight into the photo-induced dehalogenation of aryl halides catalysed by **W1a**, the reduction potentials of several aryl chlorides have been measured and these values range from −1.99 to −2.28 V *vs.* SCE (Table S2†). By considering the excited state potential E(**W1a**$^+$/**W1a***) (−1.29 V) and also the ground state potential E_{pc}(**W1a**/**W1a**$^-$) (−1.29 V), both the triplet excited tungsten photo-catalyst and one-electron reduced photo-catalyst are unable to reduce these chloro-substituted benzene substrates by outer sphere electron transfer reactions. In a recent study by Connell, Polyzos and Francis and co-workers,[39] it was found that the *in situ* reduction and hydrogenation of the ligand bound to the metal may furnish another species that is more reducing than the original one. To test if this may have occurred in our photochemical reactions, CD_2Cl_2 solutions containing both **W1a** and DIPEA were subjected to light irradiation and the reaction was monitored with ^{1}H NMR spectroscopy. The ^{1}H signals at δ 8.0–8.30 ppm assigned to the two non-equivalent hydrogen atoms on the imine bond (H–C(R)=N) of **W1a** vanished after light irradiation in the presence of excess DIPEA, indicative of the generation of new species from **W1a** (Fig. S11 and S12†). Thus, it is possible that the photoreduction of the tungsten complex afforded new species which may function as another active photocatalyst in the

reaction. However, attempts to isolate and characterize the corresponding intermediate/product have not yet been successful. Electron-primed photo-redox catalysis has recently been reported as a new strategy to enable photo-catalysts to catalyse thermodynamically challenging reactions such as reduction of aryl chlorides.[40] This strategy involves the electrochemical reduction of the photo-catalyst (PC) at a constant potential to generate a one-electron reduced PC ($PC^{\bullet -}$), which is then excited by light to generate a strong reductant ($PC^{\bullet -}$*) with reducing power comparable to that of alkali metals. Since **W1a** could be reduced photo-chemically in the presence of DIPEA to give $\mathbf{W1a}^{\bullet -}$ with a ΔO.D. at 446 nm decaying back to the baseline in ~20 μs, it may be possible that **W1a** undergoes electron-primed photoredox catalysis, though the contribution of this reaction pathway to the product yield is difficult to estimate. To examine if the dehalogenation reaction proceeded *via* the radical chain pathway, we measured the reaction quantum yield of the dehalogenation of ethyl 4-chlorobenzoate with light excitation at 420 nm. After 2 hours of light irradiation, the amount of product formed corresponded to a quantum yield of 2.7%, suggesting that this photochemical reaction is less likely to involve a radical chain mechanism.[41]

As to the reaction mechanism for borylation of aryl halides, we found that the emission of **W1a** is quenched by ethyl 4-chlorobenzoate and TBAB with k_q values of 2.3×10^5 M^{-1} s^{-1} and 5.7×10^6 M^{-1} s^{-1}, respectively, while emission quenching is not observed with B_2Pin_2. Steady state photolysis of deaerated MeCN solutions containing (i) **W1a** (2.2×10^{-5} M) and TBAB (0.1 M) and (ii) **W1a** (2.2×10^{-5} M) and ethyl 4-chlorobenzoate (0.1 M) with a blue LED has been conducted. Upon light irradiation for 7 h, the solution containing TBAB showed isosbestic UV-vis absorption spectral changes with new absorption peak maxima at 292 and 362 nm, while the solution with ethyl 4-chlorobenzoate showed a minor decrease in the absorbance at 392 nm (Fig. S14†). As the triplet excited state of **W1a** should be capable of oxidizing Br^- ($E(\mathbf{W1a}^*/\mathbf{W1a}^-) = +1.1$ V *vs.* SCE; $E(Br^{\bullet}/Br^-) = +0.8$ V *vs.* SCE[42]), **W1a*** may have been reduced to $\mathbf{W1a}^{\bullet -}$ in the reaction, though the subsequent reactions leading to product formation may be complicated and may require further study. The emissive excited state of **W1a** is ineffectively quenched by ethyl 4-chlorobenzoate with a rate constant of 2.3×10^5 M^{-1} s^{-1} only, which is consistent with the fact that the triplet excited state of **W1a** is thermodynamically not capable of reducing aryl chlorides. Given that the k_q of TBAB (5.7×10^6 M^{-1} s^{-1}) is 20 times larger than that of ethyl 4-chlorobenzoate (2.3×10^5 M^{-1} s^{-1}), under the stated reaction conditions (the ratio of TBAB to ethyl 4-chlorobenzoate is 1 : 1), reductive quenching of the triplet excited state of **W1a** by TBAB could occur upon light irradiation. The photo-stability of **W1a** in the presence of TBAB was also monitored by using ^1H NMR spectroscopy. Upon blue LED irradiation, singlet signals at 11.1 and 9.9 ppm gradually emerged. The emergence of these signals, as well as the disappearance of ^1H signals of the propylene linkage at 3.8–4.8 ppm, is indicative of **W1a** undergoing secondary reaction to give the diphenylamino-substituted salicylaldehyde. Recently other mechanisms such as two-photon-absorption,[43] *in situ* generated electron donor,[22] and homolytic C–X cleavage of aryl halide by UV light irradiation to generate aryl radicals[20] have also been proposed to be the mechanism of borylation of aryl chlorides. We found that in the absence of **W1a**, the borylated product could also be isolated in 20% yield after 12 hours (Table S5,† entry 17) and the yield increased to 68% by prolonging the reaction time to 2 days under 410 nm LED irradiation (Table S5,† entry 22). This indicates that while **W1a** indeed facilitated the borylation of aryl chloride upon light excitation, a photocatalyst-free reaction pathway (slow under the present reaction conditions) could also be involved.

For the light-induced homocoupling of 2-bromoacetophenone (Table 5, **7a**) and 1,3-dioxoisoindolin-2-yl 2-(4-isobutylphenyl)propanoate (Table 6 and **5a**), as their reduction potentials (−1.18 V and −1.14 V *vs.* SCE, respectively) are less cathodic than $E(\mathbf{W1a}^+/\mathbf{W1a}^*)$ and $E_{pc}(\mathbf{W1a}/\mathbf{W1a}^-)$ (both values are −1.29 V *vs.* SCE; Table 2), these two light-induced homocoupling reactions may proceed *via* (i) the generation of $\mathbf{W1a}^{\bullet -}$ by reductive quenching with Br^-/DIPEA, followed by the reduction of the substrate with $\mathbf{W1a}^{\bullet -}$, and/or (ii) the direct reduction of the substrate by the triplet excited state of **W1a**. The efficiency of **W1a** in catalysing these photo-induced reactions has been evaluated by drawing a comparison with the yields of the product obtained with $[Ir(ppy)_3]$ and $[Ru(bpy)_3]^{2+}$ as photocatalysts (Table 10). It was found that in most cases, the performance of **W1a** was comparable to that of $[Ir(ppy)_3]$ and significantly better than that of $[Ru(bpy)_3]^{2+}$. For example, as shown in Table 4, **W1a** catalysed light-induced reductive homocoupling of benzyl bromide to give 1,2-diphenylethane in 95% yield, but the use of $[Ir(ppy)_3]$ and $[Ru(bpy)_3]^{2+}$ as the photocatalyst only gave the product in 61% and 5% yields, respectively, under the same reaction conditions. These results confirm the competitiveness of **W1a** as an earth-abundant photocatalyst for organic transformation reactions.

The LMCT excited state of decatungstate ($W_{10}O_{32}{}^{4-}$) is known to activate C–H bonds of aliphatic alcohols *via* hydrogen-atom abstraction (HAT) giving ketones as products.[10d,j,n] For the W^{VI}-oxo complexes described herein, the LMCT transitions are high-lying in energy (~300 nm) which results in fast internal conversion to low-lying IL/ILCT excited states as revealed by fs-ta measurements, hampering the manifestation of LMCT excited state chemistry of these complexes with visible light irradiation. Nevertheless, in this work, dehydrogenation of alcohols could be observed with the use of LEDs (365 nm) as the light source. The involvement of the high-energy ^{3}LMCT excited state could not be completely excluded though we acknowledge that such an excited state is very short-lived and its formation is of low efficiency. Substrates with weaker C–H bonds, such as cyclohexa-1,4-diene and Hantzsch ester, were dehydrogenated in almost quantitative yields, suggesting that these reactions are dependent on the C–H bond strength which is consistent with the HAT pathway. However, since the reaction only occurred in the presence of oxygen, singlet oxygen and peroxy intermediates may also participate in the reaction giving the observed oxidized products. As tetraphenylporphyrin (H_2TPP) is a known photosensitizer of singlet oxygen,[44] we examined the light-induced dehydrogenation of 1-indanol by using H_2TPP as the photocatalyst. Under similar reaction conditions, the dehydrogenated

Table 10 Comparison with $[Ir(ppy)_3]$ and $[Ru(bpy)_3]^{2+a}$

Reaction	Yield		
	W1a	$[Ir(ppy)_3]$	$[Ru(bpy)_3]^{2+}$
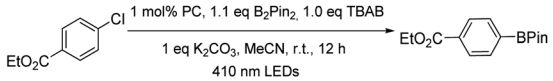	83	93	0
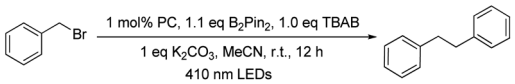	95	61	5
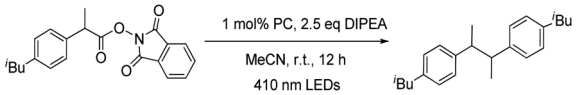	95	50	55
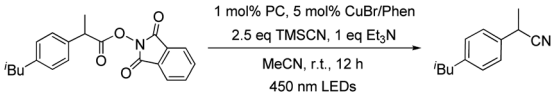	86	74	90
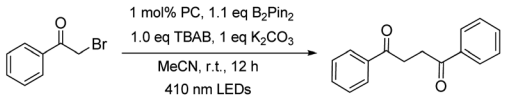	94	20	0

[a] Yields were determined by ^1H NMR spectroscopy using dibromomethane as the internal standard. Anhydrous solvents were used.

product 1-indanone was obtained in 15% yield (see Table S3,† entry 8). The capacity of **W1a** to sensitize the formation of singlet oxygen has been confirmed by measuring the emission intensity of singlet oxygen at ~1270 nm in an aerated MeCN solution of **W1a**. The singlet oxygen quantum yield of **W1a** has been estimated to be 0.06. Also, we found that addition of one molar equivalent of hydrogen peroxide into an acetonitrile solution containing 1-indanol gave 1-indanone in 45% yield (Table S3,† entry 9), suggesting that reactive oxygen species which may be formed in the reaction between triplet excited **W1a** and dissolved oxygen could eventually lead to the oxidized product 1-indanone. The involvement of the superoxide radical anion in photo-catalysis has been reported in other reactions as well.[45] It is possible that oxidation by reactive oxygen species generated from oxygen could be the major pathways for the formation of the dehydrogenated product. Regarding the mechanistic study on reductive homocoupling of benzyl bromides, DFT calculations revealed that the reduced W(VI) complex, $\mathbf{W1a}^{\bullet-}$, does not have any interaction/reaction with benzyl radicals.

Conclusion

In summary, we have developed air-stable, luminescent W(VI) complexes which could be obtained easily on the gram scale. The W(VI) complex having a diphenylamine substituent was found to catalyse visible-light-induced borylation of aryl halide, especially aryl chloride, the C–C reductive coupling reaction of benzyl bromide, the decarboxylative coupling reaction of redox-active esters of alkyl carboxylic acid, and the reductive coupling reaction of phenacyl bromide with high product yields and good tolerance to broad functional groups. It is envisioned that with further development, this class of photoluminescent W(VI) complexes could become an earth-abundant metal substitute for precious metal photosensitizers used in organic synthesis.

Conflicts of interest

There are no conflicts to declare.

Acknowledgements

This work was supported by the University Grants Committee Areas of Excellence Scheme (AoE/P-03/08), Shenzhen Science and Technology Innovation Committee (JCYJ20170412140251576 and JCYJ20180508162429786), Hong Kong Research Grants Council (HKU 17330416), China Post-doctoral Science Foundation (2018M633043) and CAS-Croucher Funding Scheme for Joint Laboratories.

References

1 (*a*) M. H. Shaw, J. Twilton and D. W. C. MacMillan, *J. Org. Chem.*, 2016, **81**, 6898; (*b*) Q. Liu and L.-Z. Wu, *Natl. Sci. Rev.*, 2017, **4**, 359; (*c*) M. Parasram and V. Gevorgyan, *Chem. Soc. Rev.*, 2017, **46**, 6227; (*d*) J. Twilton, C. Le, P. Zhang, M. H. Shaw, R. W. Evans and D. W. C. MacMillan, *Nat. Rev. Chem.*, 2017, **1**, 0052; (*e*) L. Fensterbank, J.-P. Goddard and C. Ollivier, in *Visible Light Photocatalysis in Organic Chemistry*, ed. C. Stephenson, T. Yoon and D. W. C. MacMillan, Wiley-VCH Verlag GmbH & Co.KGaA, Weinheim, 2018; (*f*) C. B. Larsen

and O. S. Wenger, *Chem. – Eur. J.*, 2018, **24**, 2039; (*g*) L. Marzo, S. K. Pagire, O. Reiser and B. Konig, *Angew. Chem., Int. Ed.*, 2018, **57**, 10034; (*h*) R. C. McAtee, E. J. McClain and C. R. J. Stephenson, *Trends Chem.*, 2019, **1**, 111; (*i*) F. Glaser and O. S. Wenger, *Coord. Chem. Rev.*, 2020, **405**, 213129; (*j*) B. M. Hockin, C. Li, N. Robertson and E. Zysman-Colman, *Catal. Sci. Technol.*, 2019, **9**, 889; (*k*) C. Förster and K. Heinze, *Chem. Soc. Rev.*, 2020, **49**, 1057.

2 (*a*) C. O. Dietrich-Buchecker, P. A. Marnot, J.-P. Sauvage, J. R. Kirchhoff and D. R. McMillin, *J. Chem. Soc., Chem. Commun.*, 1983, 513; (*b*) J.-M. Kern and J.-P. Sauvage, *J. Chem. Soc., Chem. Commun.*, 1987, 546; (*c*) D. Li, C.-M. Che, H.-L. Kwong and V. W.-W. Yam, *J. Chem. Soc., Dalton Trans.*, 1992, 3325; (*d*) D. G. Cuttell, S.-M. Kuang, P. E. Fanwick, D. R. McMillin and R. A. Walton, *J. Am. Chem. Soc.*, 2002, **124**, 6; (*e*) B. Wang, D. P. Shelar, X.-Z. Han, T.-T. Li, X. Guan, W. Lu, K. Liu, Y. Chen, W.-F. Fu and C.-M. Che, *Chem. – Eur. J.*, 2015, **21**, 1184; (*f*) M. Knorn, T. Rawner, R. Czerwieniec and O. Reiser, *ACS Catal.*, 2015, **5**, 5186; (*g*) M. M. Cetin, R. T. Hodson, C. R. Hart, D. B. Cordes, M. Findlater, D. J. Casadonte Jr, A. F. Cozzolino and M. F. Mayer, *Dalton Trans.*, 2017, **46**, 6553.

3 (*a*) M. Grubel, I. Bosque, P. J. Altmann, T. Bach and C. R. Hess, *Chem. Sci.*, 2018, **9**, 3313; (*b*) L. A. Buldt, C. B. Larsen and O. S. Wenger, *Chem. – Eur. J.*, 2017, **23**, 8577; (*c*) S. Malzkuhn and O. S. Wenger, *Coord. Chem. Rev.*, 2018, **359**, 52; (*d*) C.-H. Lim, M. Kudisch, B. Liu and G. M. Miyake, *J. Am. Chem. Soc.*, 2018, **140**, 7667; (*e*) X. Shen, Y. Li, Z. Wen, S. Cao, X. Hou and L. Gong, *Chem. Sci.*, 2018, **9**, 4562; (*f*) B. J. Shields, B. Kudisch, G. D. Scholes and A. G. Doyle, *J. Am. Chem. Soc.*, 2018, **140**, 3035; (*g*) R. C. G. Frem, A. C. Massabni, A. M. G. Massabni and A. E. Mauro, *Inorg. Chim. Acta*, 1997, **255**, 53; (*h*) H. Kunkely and A. Vogler, *Inorg. Chem. Commun.*, 2000, **3**, 143.

4 (*a*) Y. Zhang, J. L. Petersen and C. Milsmann, *J. Am. Chem. Soc.*, 2016, **138**, 13115; (*b*) Y. Zhang, T. S. Lee, J. L. Petersen and C. Milsmann, *J. Am. Chem. Soc.*, 2018, **140**, 5934.

5 (*a*) L. A. Büldt, X. Guo, A. Prescimone and O. S. Wenger, *Angew. Chem., Int. Ed.*, 2016, **55**, 11247; (*b*) P. Herr, F. Glaser, L. A. Büldt, C. B. Larsen and O. S. Wenger, *J. Am. Chem. Soc.*, 2019, **141**, 14394.

6 (*a*) S. M. Stevenson, M. P. Shores and E. M. Ferreira, *Angew. Chem., Int. Ed.*, 2015, **54**, 6506; (*b*) R. F. Higgins, S. M. Fatur, S. G. Shepard, S. M. Stevenson, D. J. Boston, E. M. Ferreira, N. H. Damrauer, A. K. Rappé and M. P. Shores, *J. Am. Chem. Soc.*, 2016, **138**, 5451; (*c*) S. Otto, A. M. Nauth, E. Ermilov, N. Scholz, A. Friedrich, U. Resch-Genger, S. Lochbrunner, T. Opatz and K. Heinze, *ChemPhotoChem*, 2017, **1**, 344; (*d*) S. M. Stevenson, R. F. Higgins, M. P. Shores and E. M. Ferreira, *Chem. Sci.*, 2017, **8**, 654.

7 (*a*) P. Chábera, Y. Z. Liu, O. Prakash, E. Thyrhaug, A. El Nahhas, A. Honarfar, S. Essen, L. A. Fredin, T. C. B. Harlang, K. S. Kjær, K. Handrup, F. Ericson, H. Tatsuno, K. Morgan, J. Schnadt, L. Häggström, T. Ericsson, A. Sobkowiak, S. Lidin, P. Huang, S. Styring, J. Uhlig, J. Bendix, R. Lomoth, V. Sundström, P. Persson and K. Wärnmark, *Nature*, 2017, **543**, 695; (*b*) K. S. Kjær, N. Kaul, O. Prakash, P. Chábera, N. W. Rosemann, A. Honarfar, O. Gordivska, L. A. Fredin, K.-E. Bergquist, L. Häggström, T. Ericsson, L. Lindh, A. Yartsev, S. Styring, P. Huang, J. Uhlig, J. Bendix, D. Strand, V. Sundström, P. Persson, R. Lomoth and K. Wärnmark, *Science*, 2019, **363**, 249; (*c*) A. Gualandi, M. Marchini, L. Mengozzi, M. Natali, M. Lucarini, P. Ceroni and P. G. Cozzi, *ACS Catal.*, 2015, **5**, 5927; (*d*) J. Zhang, D. Campolo, F. Dumur, P. Xiao, J. P. Fouassier, D. Gigmes and J. Lalevée, *J. Polym. Sci., Part A: Polym. Chem.*, 2015, **53**, 42; (*e*) J. Zhang, D. Campolo, F. Dumur, P. Xiao, J. P. Fouassier, D. Gigmes and J. Lalevée, *ChemCatChem*, 2016, **8**, 2227; (*f*) P. Zimmer, P. Müller, L. Burkhardt, R. Schepper, A. Neuba, J. Steube, F. Dietrich, U. Flörke, S. Mangold, M. Gerhards and M. Bauer, *Eur. J. Inorg. Chem.*, 2017, 1504.

8 (*a*) H. Yin, P. J. Carroll, J. M. Anna and E. J. Schelter, *J. Am. Chem. Soc.*, 2015, **137**, 9234; (*b*) J.-J. Guo, A. Hu, Y. Chen, J. Sun, H. Tang and Z. Zuo, *Angew. Chem., Int. Ed.*, 2016, **55**, 15319; (*c*) H. Yin, P. J. Carroll, B. C. Manor, J. M. Anna and E. J. Schelter, *J. Am. Chem. Soc.*, 2016, **138**, 5984; (*d*) H. Yin, Y. Jin, J. E. Hertzog, K. C. Mullane, P. J. Carroll, B. C. Manor, J. M. Anna and E. J. Schelter, *J. Am. Chem. Soc.*, 2016, **138**, 16266; (*e*) A. Hu, Y. Chen, J.-J. Guo, N. Yu, Q. An and Z. Zuo, *J. Am. Chem. Soc.*, 2018, **140**, 13580; (*f*) A. Hu, J.-J. Guo, H. Pan, H. Tang, Z. Gao and Z. Zuo, *J. Am. Chem. Soc.*, 2018, **140**, 1612; (*g*) A. Hu, J.-J. Guo, H. Pan and Z. Zuo, *Science*, 2018, **361**, 668; (*h*) T. C. Jenks, M. D. Bailey, J. L. Hovey, S. Fernando, G. Basnayake, M. E. Cross, W. Li and M. J. Allen, *Chem. Sci.*, 2018, **9**, 1273; (*i*) Y. Qiao, Q. Yang and E. J. Schelter, *Angew. Chem., Int. Ed.*, 2018, **57**, 10999.

9 (*a*) Y.-Q. Wu, G.-X. Lu and S.-B. Li, *Acta Chim. Sin.*, 2004, **62**, 1134; (*b*) Z. Chen and J. Su, *J. Jiangsu Univ.*, 2005, **26**, 57; (*c*) Y. Cui, H. Li and K. Zhang, *Preparation of tungsten trioxide photocatalyst and its Application*, Chemical Industry Press. Co. Ltd., Beijing, 2012; (*d*) J. G. West and E. J. Sorensen, *Isr. J. Chem.*, 2017, **57**, 259; (*e*) K. Suzuki, N. Mizuno and K. Yamaguchi, *ACS Catal.*, 2018, **8**, 10809; (*f*) Z. Yuan, H. Yang, N. Malik, M. Čolović, D. S. Weber, D. Wilson, F. Bénard, R. E. Martin, J. J. Warren, P. Schaffer and R. Britton, *ACS Catal.*, 2019, **9**, 8276.

10 (*a*) C. L. Hill, *Synlett*, 1995, 127; (*b*) A. Maldotti, R. Amadelli, V. Carassiti and A. Molinari, *Inorg. Chim. Acta*, 1997, **256**, 309; (*c*) D. Dondi, M. Fagnoni, A. Molinari, A. Maldotti and A. Albini, *Chem. – Eur. J.*, 2004, **10**, 142; (*d*) A. Maldotti, A. Molinari and F. Bigi, *J. Catal.*, 2008, **253**, 312; (*e*) M. D. Tzirakis and M. Orfanopoulos, *J. Am. Chem. Soc.*, 2009, **131**, 4063; (*f*) M. D. Tzirakis and M. Orfanopoulos, *Angew. Chem., Int. Ed.*, 2010, **49**, 5891; (*g*) S. D. Halperin, H. Fan, S. Chang, R. E. Martin and R. Britton, *Angew. Chem., Int. Ed.*, 2014, **53**, 4690; (*h*) M. Okada, T. Fukuyama, K. Yamada, I. Ryu, D. Ravelli and M. Fagnoni, *Chem. Sci.*, 2014, **5**, 2893; (*i*) S. D. Halperin, D. Kwon, M. Holmes, E. L. Regalado, L.-C. Campeau, D. A. DiRocco and

R. Britton, *Org. Lett.*, 2015, **17**, 5200; (*j*) J. G. West, D. Huang and E. J. Sorensen, *Nat. Commun.*, 2015, **6**, 10093; (*k*) K. Yamada, M. Okada, T. Fukuyama, D. Ravelli, M. Fagnoni and I. Ryu, *Org. Lett.*, 2015, **17**, 1292; (*l*) M. Meanwell, M. B. Nodwell, R. E. Martin and R. Britton, *Angew. Chem., Int. Ed.*, 2016, **55**, 13244; (*m*) J. J. Murphy, D. Bastida, S. Paria, M. Fagnoni and P. Melchiorre, *Nature*, 2016, **532**, 218; (*n*) D. J. Abrams, J. G. West and E. J. Sorensen, *Chem. Sci.*, 2017, **8**, 1954; (*o*) M. C. Quattrini, S. Fujii, K. Yamada, T. Fukuyama, D. Ravelli, M. Fagnoni and I. Ryu, *Chem. Commun.*, 2017, **53**, 2335; (*p*) D. M. Schultz, F. Lévesque, D. A. DiRocco, M. Reibarkh, Y. Ji, L. A. Joyce, J. F. Dropinski, H. Sheng, B. D. Sherry and I. W. Davies, *Angew. Chem., Int. Ed.*, 2017, **56**, 15274; (*q*) G. Laudadio, S. Govaerts, Y. Wang, D. Ravelli, H. F. Koolman, M. Fagnoni, S. W. Djuric and T. Noël, *Angew. Chem., Int. Ed.*, 2018, **57**, 4078; (*r*) M. Meanwell, J. Lehmann, M. Eichenberger, R. E. Martin and R. Britton, *Chem. Commun.*, 2018, **54**, 9985; (*s*) I. B. Perry, T. F. Brewer, P. J. Sarver, D. M. Schultz, D. A. DiRocco and D. W. C. MacMillan, *Nature*, 2018, **560**, 70; (*t*) Z. Yuan, M. B. Nodwell, H. Yang, N. Malik, H. Merkens, F. Bénard, R. E. Martin, P. Schaffer and R. Britton, *Angew. Chem., Int. Ed.*, 2018, **57**, 12733; (*u*) V. I. Supranovich, V. V. Levin and A. D. Dilman, *Org. Lett.*, 2019, **21**, 4271; (*v*) H.-B. Yang, A. Feceu and D. B. C. Martin, *ACS Catal.*, 2019, **9**, 5708.

11 D. C. Duncan, T. L. Netzel and C. L. Hill, *Inorg. Chem.*, 1995, **34**, 4640.

12 (*a*) K. R. Mann, M. Cimolino, G. L. Geoffroy, G. S. Hammond, A. A. Orio, G. Albertin and H. B. Gray, *Inorg. Chim. Acta*, 1976, **16**, 97; (*b*) K. R. Mann, H. B. Gray and G. S. Hammond, *J. Am. Chem. Soc.*, 1977, **99**, 306; (*c*) W. Sattler, L. M. Henling, J. R. Winkler and H. B. Gray, *J. Am. Chem. Soc.*, 2015, **137**, 1198; (*d*) K. Takematsu, S. A. M. Wehlin, W. Sattler, J. R. Winkler and H. B. Gray, *Dalton Trans.*, 2017, **46**, 13188.

13 K.-T. Yeung, W.-P. To, C. Sun, G. Cheng, C. Ma, G. S. M. Tong, C. Yang and C.-M. Che, *Angew. Chem., Int. Ed.*, 2017, **56**, 133.

14 K. Li, Q. Wan, C. Yang, X.-Y. Chang, K.-H. Low and C.-M. Che, *Angew. Chem., Int. Ed.*, 2018, **57**, 14129.

15 K.-T. Chan, T.-L. Lam, D. Yu, L. Du, D. L. Phillips, C.-L. Kwong, G. S. M. Tong, G. Cheng and C.-M. Che, *Angew. Chem., Int. Ed.*, 2019, **58**, 14896.

16 W.-P. To, D. Zhou, G. S. M. Tong, G. Cheng, C. Yang and C.-M. Che, *Angew. Chem., Int. Ed.*, 2017, **56**, 14036.

17 A. M. Srivastava and J. F. Ackerman, *Mater. Res. Bull.*, 1999, **34**, 1397.

18 (*a*) W.-P. To, K. T. Chan, G. S. M. Tong, C. Ma, W.-M. Kwok, X. Guan, K.-H. Low and C.-M. Che, *Angew. Chem., Int. Ed.*, 2013, **52**, 6648; (*b*) G. Cheng, S. C. F. Kui, W.-H. Ang, M.-Y. Ko, P.-K. Chow, C.-L. Kwong, C.-C. Kwok, C. Ma, X. Guan, K.-H. Low, S.-J. Su and C.-M. Che, *Chem. Sci.*, 2014, **5**, 4819; (*c*) P.-K. Chow, G. Cheng, G. S. M. Tong, W.-P. To, W.-L. Kwong, K.-H. Low, C.-C. Kwok, C. Ma and C.-M. Che, *Angew. Chem., Int. Ed.*, 2015, **54**, 2084; (*d*) K. T. Chan, G. S. M. Tong, W.-P. To, C. Yang, L. Du, D. L. Phillips and C.-M. Che, *Chem. Sci.*, 2017, **8**, 2352.

19 (*a*) N. Miyaura and A. Suzuki, *Chem. Rev.*, 1995, **95**, 2457; (*b*) A. Suzuki, *Angew. Chem., Int. Ed.*, 2011, **50**, 6722; (*c*) J. Yamaguchi, A. D. Yamaguchi and K. Itami, *Angew. Chem., Int. Ed.*, 2012, **51**, 8960; (*d*) L. Xu, S. Zhang and P. Li, *Chem. Soc. Rev.*, 2015, **44**, 8848.

20 (*a*) K. Chen, M. S. Cheung, Z. Lin and P. Li, *Org. Chem. Front.*, 2016, **3**, 875; (*b*) K. Chen, S. Zhang, P. He and P. Li, *Chem. Sci.*, 2016, **7**, 3676; (*c*) A. M. Mfuh, J. D. Doyle, B. Chhetri, H. D. Arman and O. V. Larionov, *J. Am. Chem. Soc.*, 2016, **138**, 2985; (*d*) A. M. Mfuh, V. T. Nguyen, B. Chhetri, J. E. Burch, J. D. Doyle, V. N. Nesterov, H. D. Arman and O. V. Larionov, *J. Am. Chem. Soc.*, 2016, **138**, 8408; (*e*) W. Liu, X. Yang, Y. Gao and C.-J. Li, *J. Am. Chem. Soc.*, 2017, **139**, 8621.

21 (*a*) M. Jiang, H. Yang and H. Fu, *Org. Lett.*, 2016, **18**, 5248; (*b*) A. Nitelet, D. Thevenet, B. Schiavi, C. Hardouin, J. Fournier, R. Tamion, X. Pannecoucke, P. Jubault and T. Poisson, *Chem. – Eur. J.*, 2019, **25**, 3262.

22 (*a*) L. Zhang and L. Jiao, *J. Am. Chem. Soc.*, 2017, **139**, 607; (*b*) L. Zhang and L. Jiao, *J. Am. Chem. Soc.*, 2019, **141**, 9124.

23 K. Hironaka, S. Fukuzumi and T. Tanaka, *J. Chem. Soc., Perkin Trans. 2*, 1984, 1705.

24 G. Park, S. Y. Yi, J. Jung, E. J. Cho and Y. You, *Chem. – Eur. J.*, 2016, **22**, 17790.

25 (*a*) S. Fukuzumi, S. Mochizuki and T. Tanaka, *J. Phys. Chem.*, 1990, **94**, 722; (*b*) J. Jung, J. Kim, G. Park, Y. You and E. J. Cho, *Adv. Synth. Catal.*, 2016, **358**, 74; (*c*) M. Hou, L. Lin, X. Chai, X. Zhao, B. Qiao and Z. Jiang, *Chem. Sci.*, 2019, **10**, 6629; (*d*) X. Zhu, Y. Lin, Y. Sun, M. C. Beard and Y. Yan, *J. Am. Chem. Soc.*, 2019, **141**, 733.

26 (*a*) K. Okada, K. Okamoto and M. Oda, *J. Am. Chem. Soc.*, 1988, **110**, 8736; (*b*) K. Okada, K. Okamoto, N. Morita, K. Okubo and M. Oda, *J. Am. Chem. Soc.*, 1991, **113**, 9401; (*c*) M. Zlotorzynska and G. M. Sammis, *Org. Lett.*, 2011, **13**, 6264; (*d*) C. R. Jamison and L. E. Overman, *Acc. Chem. Res.*, 2016, **49**, 1578; (*e*) J. Schwarz and B. König, *Green Chem.*, 2016, **18**, 4743; (*f*) S. Murarka, *Adv. Synth. Catal.*, 2018, **360**, 1735.

27 K. Okada, K. Okubo, N. Morita and M. Oda, *Chem. Lett.*, 1993, **22**, 2021.

28 W. Sha, L. Deng, S. Ni, H. Mei, J. Han and Y. Pan, *ACS Catal.*, 2018, **8**, 7489.

29 K. Okada, K. Okamoto and M. Oda, *J. Chem. Soc., Chem. Commun.*, 1989, 1636.

30 W.-T. Jiang, S. Yang, M.-Y. Xu, X.-Y. Xie and B. Xiao, *Chem. Sci.*, 2020, **11**, 488.

31 R. Mao, J. Balon and X. Hu, *Angew. Chem., Int. Ed.*, 2018, **57**, 9501.

32 (*a*) Z.-J. Wang, J.-J. Lv, R.-N. Yi, M. Xiao, J.-J. Feng, Z.-W. Liang, A.-J. Wang and X. Xu, *Adv. Synth. Catal.*, 2018, **360**, 932; (*b*) Y. Liu, S. Xiao, Y. Qi and F. Du, *Chem.–Asian J.*, 2017, **12**, 673; (*c*) B. J. Fallon, V. Corcé, M. Amatore, C. Aubert, F. Chemla, F. Ferreira, A. Perez-Luna and M. Petit, *New J. Chem.*, 2016, **40**, 9912; (*d*) K. Sato, Y. Inoue, T. Mori, A. Sakaue, A. Tarui, M. Omote, I. Kumadaki and

A. Ando, *Org. Lett.*, 2014, **16**, 3756; (*e*) S.-H. Kim and R. D. Rieke, *J. Org. Chem.*, 2000, **65**, 2322.

33 D. Wang, N. Zhu, P. Chen, Z. Lin and G. Liu, *J. Am. Chem. Soc.*, 2017, **139**, 15632.

34 (*a*) H. Kim and C. Lee, *Angew. Chem., Int. Ed.*, 2012, **51**, 12303; (*b*) G. Revol, T. McCallum, M. Morin, F. Gagosz and L. Barriault, *Angew. Chem., Int. Ed.*, 2013, **52**, 13342; (*c*) S. M. Senaweera, A. Singh and J. D. Weaver, *J. Am. Chem. Soc.*, 2014, **136**, 3002; (*d*) M. Häring, R. Pérez-Ruiz, A. Jacobi von Wangelin and D. D. Díaz, *Chem. Commun.*, 2015, **51**, 16848; (*e*) S. O. Poelma, G. L. Burnett, E. H. Discekici, K. M. Mattson, N. J. Treat, Y. Luo, Z. M. Hudson, S. L. Shankel, P. G. Clark, J. W. Kramer, C. J. Hawker and J. Read de Alaniz, *J. Org. Chem.*, 2016, **81**, 7155; (*f*) B. Michelet, C. Deldaele, S. Kajouj, C. Moucheron and G. Evano, *Org. Lett.*, 2017, **19**, 3576; (*g*) J. I. Bardagi, I. Ghosh, M. Schmalzbauer, T. Ghosh and B. König, *Eur. J. Org. Chem.*, 2018, 34; (*h*) T. U. Connell, C. L. Fraser, M. L. Czyz, Z. M. Smith, D. J. Hayne, E. H. Doeven, J. Agugiaro, D. J. D. Wilson, J. L. Adcock, A. D. Scully, D. E. Gómez, N. W. Barnett, A. Polyzos and P. S. Francis, *J. Am. Chem. Soc.*, 2019, **141**, 17646; (*i*) A. Steiner, J. D. Williams, J. A. Rincón, O. de Frutos, C. Mateos and C. O. Kappe, *Eur. J. Org. Chem.*, 2019, 5807.

35 W. Kong, C. Yu, H. An and Q. Song, *Org. Lett.*, 2018, **20**, 349.

36 (*a*) N. Ma, W. Shi, R. Zhang, Z. Zhu and Z. Jiang, *Tetrahedron Lett.*, 2011, **52**, 718; (*b*) M. Nakajima, E. Fava, S. Loescher, Z. Jiang and M. Rueping, *Angew. Chem., Int. Ed.*, 2015, **54**, 8828; (*c*) S. Okamoto, K. Kojiyama, H. Tsujioka and A. Sudo, *Chem. Commun.*, 2016, **52**, 11339; (*d*) A. Gualandi, G. Rodeghiero, E. Della Rocca, F. Bertoni, M. Marchini, R. Perciaccante, T. P. Jansen, P. Ceroni and P. G. Cozzi, *Chem. Commun.*, 2018, **54**, 10044; (*e*) T. Kohlmann, C. Kerzig and M. Goez, *Chem. – Eur. J.*, 2019, **25**, 9991.

37 D. Saberi and H. Hashemi, *Catal. Commun.*, 2018, **106**, 50.

38 (*a*) J. D. Nguyen, J. W. Tucker, M. D. Konieczynska and C. R. J. Stephenson, *J. Am. Chem. Soc.*, 2011, **133**, 4160; (*b*) C.-J. Wallentin, J. D. Nguyen, P. Finkbeiner and C. R. J. Stephenson, *J. Am. Chem. Soc.*, 2012, **134**, 8875.

39 T. U. Connell, C. L. Fraser, M. L. Czyz, Z. M. Smith, D. J. Hayne, E. H. Doeven, J. Agugiaro, D. J. D. Wilson, J. L. Adcock, A. D. Scully, D. E. Gómes, N. W. Barnett, A. Polyzos and P. S. Francis, *J. Am. Chem. Soc.*, 2019, **141**, 17646.

40 (*a*) L. Capaldo, L. L. Quadri and D. Ravelli, *Angew. Chem., Int. Ed.*, 2019, **58**, 17508; (*b*) H. Huang, Z. M. Strater, M. Rauch, J. Shee, T. J. Sisto, C. Nuckolls and T. H. Lambert, *Angew. Chem., Int. Ed.*, 2019, **58**, 13318; (*c*) H. Yan, Z.-W. Hou and H.-C. Xu, *Angew. Chem., Int. Ed.*, 2019, **58**, 4592; (*d*) N. G. W. Cowper, C. P. Chernowsky, O. P. Williams and Z. K. Wickens, *J. Am. Chem. Soc.*, 2020, **142**, 2093; (*e*) H. Kim, H. Kim, T. H. Lambert and S. Lin, *J. Am. Chem. Soc. Chem*, 2020, **142**, 2087.

41 M. A. Cismesia and T. P. Yoon, *Chem. Sci.*, 2015, **6**, 5426.

42 Z. Wang, Q. Liu, X. Ji, G.-J. Deng and H. Huang, *ACS Catal.*, 2020, **10**, 154.

43 (*a*) I. Ghosh, T. Ghosh, J. I. Bardagi and B. König, *Science*, 2014, **346**, 725; (*b*) C. Kerzig and O. S. Wenger, *Chem. Sci.*, 2019, **10**, 11023; (*c*) F. Glaser, C. Kerzig and O. S. Wenger, *Angew. Chem., Int. Ed.*, 2020, **59**, DOI: 10.1002/anie.201915762.

44 M. C. DeRosa and R. J. Crutchley, *Coord. Chem. Rev.*, 2002, **233–234**, 351.

45 (*a*) Y.-Q. Zou, L.-Q. Lu, L. Fu, N.-J. Chang, J. Rong, J.-R. Chen and W.-J. Xiao, *Angew. Chem., Int. Ed.*, 2011, **50**, 7171; (*b*) Y.-Q. Zou, J.-R. Chen, X.-P. Liu, L.-Q. Lu, R. L. Davis, K. A. Jørgensen and W.-J. Xiao, *Angew. Chem., Int. Ed.*, 2012, **51**, 784.